1521-0103/12/3432-307–315$25.00
THE JOURNAL OF PHARMACOLOGY AND EXPERIMENTAL THERAPEUTICS Vol. 343, No. 2
Copyright © 2012 by The American Society for Pharmacology and Experimental Therapeutics 195255/3799610
JPET 343:307–315, 2012

CYP2A6- and CYP2A13-Catalyzed Metabolism of the Nicotine $\Delta^{5'(1')}$Iminium Ion

Linda B. von Weymarn, Cassandra Retzlaff, and Sharon E. Murphy

Department of Biochemistry, Molecular Biology, and Biophysics and Masonic Cancer Center, University of Minnesota, Minneapolis, Minnesota

Received April 4, 2012; accepted August 2, 2012

ABSTRACT

Nicotine, the major addictive agent in tobacco, is metabolized primarily by CYP2A6-catalyzed oxidation. The product of this reaction, 5′-hydroxynicotine, is in equilibrium with the nicotine $\Delta^{5'(1')}$iminium ion and is further metabolized to cotinine. We reported previously that both CYP2A6 and the closely related extrahepatic enzyme CYP2A13 were inactivated during nicotine metabolism; however, inactivation occurred after metabolism was complete. This led to the hypothesis that oxidation of a nicotine metabolite, possibly the nicotine $\Delta^{5'(1')}$iminium ion, was responsible for generating the inactivating species. In the studies presented here, we confirm that the nicotine $\Delta^{5'(1')}$iminium ion is an inactivator of both CYP2A6 and CYP2A13, and inactivation depends on time, concentration, and the presence of NADPH. Inactivation was not reversible and was accompanied by a parallel loss in spectrally active protein, as measured by reduced CO spectra. These data are consistent with the characterization of the nicotine $\Delta^{5'(1')}$iminium ion as a mechanism-based inactivator of both CYP2A13 and CYP2A6. We also confirm that both CYP2A6 and CYP2A13 catalyze the metabolism of the nicotine $\Delta^{5'(1')}$iminium ion to cotinine and provide evidence that both enzymes catalyze the sequential metabolism of the nicotine $\Delta^{5'(1')}$iminium ion. That is, a fraction of the cotinine formed may not be released from the enzyme before further oxidation to 3′-hydroxycotinine.

Introduction

Nicotine, the major addictive agent in tobacco, is metabolized primarily by cytochrome P450-mediated oxidation (Hukkanen et al., 2005). The product of this reaction, 5′-hydroxynicotine, is in equilibrium with the nicotine $\Delta^{5'(1')}$iminium ion and is further metabolized to cotinine. Subsequently, cotinine is metabolized to *trans*-3′-hydroxycotinine (3HCOT) (Fig. 1). The conversion of nicotine to cotinine and 3′-hydroxycotinine typically accounts for 70 to 80% of the metabolism of nicotine in smokers (Hukkanen et al., 2005). The cytosolic enzyme aldehyde oxidase catalyzes the oxidation of the $\Delta^{5'(1')}$iminium ion to cotinine (Brandänge and Lindblom, 1979; Gorrod and Hibberd, 1982); however, Shigenaga et al. (1988) reported that the conversion of the nicotine $\Delta^{5'(1')}$iminium ion to cotinine occurs in rabbit liver microsomal fractions. More recently, we have reported that cotinine is a product of CYP2A6- and CYP2A13-catalyzed nicotine metabolism (Murphy et al., 2005; von Weymarn et al., 2006).

The hepatic enzyme CYP2A6 is the primary catalyst of nicotine 5′ oxidation in humans (Hukkanen et al., 2005). The closely related enzyme CYP2A13, expressed in the lung (Su et al., 2000), is a somewhat better catalyst of this reaction (Bao et al., 2005; Murphy, et al., 2005). The role of CYP2A13 in the metabolism of nicotine in vivo is as yet unknown. Both CYP2A6 and CYP2A13 also catalyze the oxidation of cotinine. The products of these reactions include *trans*-3′-hydroxycotinine, 5′-hydroxycotinine (5HCOT), and *N*-(hydroxymethyl)norcotinine (NHCOT) (Fig. 1) (Nakajima et al., 1996; Murphy et al., 1999; Brown et al., 2005). In contrast to what is observed in smokers, *trans*-3′-hydroxycotinine is not the primary product of CYP2A6- and CYP2A13-mediated cotinine metabolism in vitro (Murphy et al., 1999; Brown et al., 2005). The major product of CYP2A6-mediated cotinine metabolism is *N*-(hydroxymethyl)norcotinine, and 5′-hydroxycotinine is the primary product of CYP2A13-catalyzed metabolism (Brown et al., 2005).

CYP2A6 and CYP2A13, which are 94% identical, metabolize many common substrates, but the product distribution and rates of the reactions often differ. For example,

This work was supported by the National Institutes of Health National Cancer Institute [Grant CA-84529].

Article, publication date, and citation information can be found at http://jpet.aspetjournals.org.

http://dx.doi.org/10.1124/jpet.112.195255.

ABBREVIATIONS: 3HCOT, 3′-hydroxycotinine; 5HCOT, 5′-hydroxycotinine; NHCOT, *N*-(hydroxymethyl)norcotinine; NCOT, norcotinine; P450, cytochrome P450; (*S*)-NNN, (*S*)-*N*′-nitrosonornicotine; TFA, triflouroacetic acid; β-nicotyrine, 1-methyl-4-(3-pyridinyl)pyrrole; HPLC, high-performance liquid chromatography; LC, liquid chromatography; MS, mass spectrometry; MS/MS, tandem MS; S.A., specific activity.

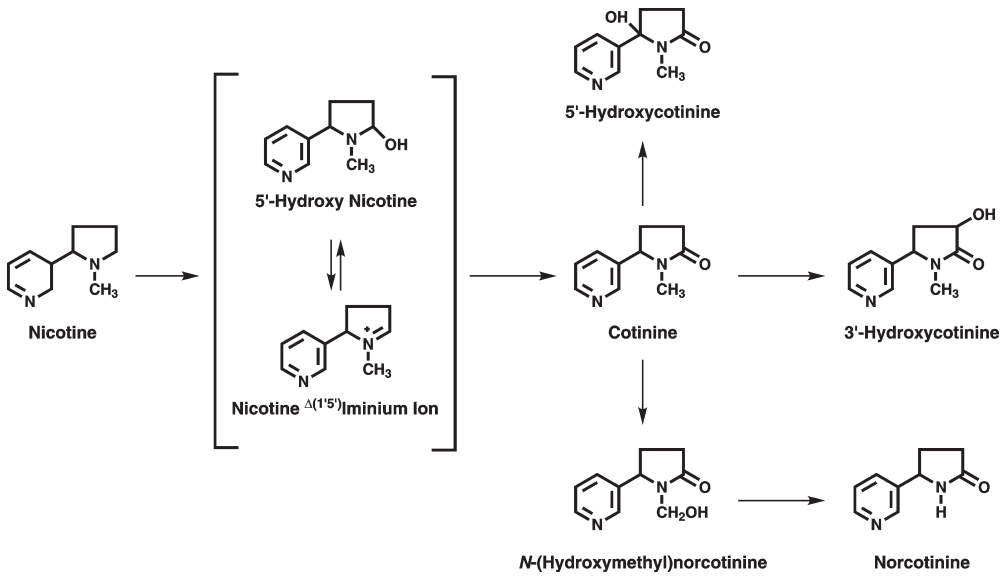

Fig. 1. Primary pathways of nicotine oxidation.

CYP2A6 exclusively catalyzes the 7-hydroxylation of coumarin, whereas CYP2A13 catalyzes both the 7-hydroxylation and the 3,4-epoxidation of coumarin (von Weymarn and Murphy, 2003; Schlicht et al., 2009). Metabolism of the tobacco-specific carcinogen 4-(methylnitrosamino)-1-(3-pyridyl)-1-butanone by CYP2A6 and CYP2A13 generates a similar distribution of products. However, the catalytic activity (V_{max}/K_m) of CYP2A13-mediated 4-(methylnitrosamino)-1-(3-pyridyl)-1-butanone (NNK) metabolism is more than 200-fold greater than that of CYP2A6 (Jalas et al., 2005). The significantly larger active site of CYP2A13 relative to CYP2A6 (Yano et al., 2005; Smith et al., 2007) is likely to contribute to some of these differences.

We reported previously that both CYP2A6 and CYP2A13 were inactivated during nicotine metabolism (von Weymarn et al., 2006). The irreversible inactivation of the two enzymes by nicotine was time-, concentration-, and NADPH-dependent. However, the majority of the inactivation occurred after nicotine metabolism was complete, leading us to suggest that a secondary metabolite of nicotine may be responsible. A likely precursor to the inactivating species is the primary product of CYP2A6- and CYP2A13-catalyzed nicotine metabolism, the nicotine $\Delta^{5'(1')}$iminium ion. We report here that the nicotine $\Delta^{5'(1')}$iminium ion inactivates both CYP2A6 and CYP2A13 in a time-, concentration-, and NADPH-dependent manner. In addition, we characterize the products of CYP2A6- and CYP2A13-catalyzed nicotine $\Delta^{5'(1')}$iminium ion metabolism and present data supporting the sequential metabolism of the iminium ion to *trans*-3′-hydroxycotinine by CYP2A13. That is, we suggest that a portion of the primary metabolite, cotinine, is oxidized to *trans*-3′-hydroxycotinine before being released from the active site.

Materials and Methods

Chemicals and Enzymes. Nicotine $\Delta^{5'(1')}$iminium ion was synthesized as described previously (Peterson et al., 1987). [5-^{3}H]nicotine $\Delta^{5'(1')}$iminium ion was prepared enzymatically from [5-^{3}H](*S*)-nicotine as described below. *N*-(hydroxymethyl)norcotinine was synthesized as described previously (Brown et al., 2005). The [5-^{3}H](*S*)-nicotine was prepared from (*S*)-5′-bromonicotine by Moravek Biochemicals (Brea, CA) and purified by HPLC as described previously (Murphy et al., 2005). Cotinine *N*-oxide, norcotinine, 5′-hydroxycotinine, *cis*- and *trans*-3′-hydroxycotinine, and (*S*)- NNN were purchased from Toronto Research Chemicals Inc. (North York, ON, Canada). (*S*)-nicotine, cotinine, nornicotine, 7-hydroxycoumarin, coumarin, dilauroyl-L-α-phosphatidylcholine, NADPH, bovine serum albumin, catalase, and all other biochemical reagents were obtained from Sigma-Aldrich (St. Louis, MO) and were of analytical grade. TFA and dialysis cassettes were obtained from Pierce (Rockford, IL). The d_9-*trans*-3′-hydroxycotinine was a kind gift from Dr. Payton Jacob (University of California, San Francisco, CA). The enzymes used in this study were expressed in *Escherichia coli* and purified according to previously published protocols (Hanna et al., 1998; Kent et al., 1999; Soucek, 1999; von Weymarn et al., 2005).

Preparation of Tritium-Labeled Nicotine $\Delta^{5'(1')}$Iminium Ion. Purified CYP2A13 (100 pmol) was reconstituted with rat NADPH-cytochrome P450 oxidoreductase (reductase) (100 pmol) and dilauroyl-L-α-phosphatidylcholine (30 μg) for 45 min at 4°C. The reconstituted enzyme mixture was incubated with [5-^{3}H](*S*)-nicotine (150 μCi; 20 μCi/nmol), catalase (60 units/μl), and an NADPH-generating system (0.4 mM $NADP^+$, 10 mM glucose 6-phosphate, and 0.4 units/ml glucose phosphate dehydrogenase) in 200 μl of Tris buffer (100 mM; pH 7.4) for 10 min at 30°C. The reaction was terminated by the addition of 20 μl of 15% trichloroacetic acid and centrifuged for 10 min at 1500*g*. The [5-^{3}H]nicotine $\Delta^{5'(1')}$iminium ion was purified by collection from HPLC system I (see below). The fractions containing nicotine $\Delta^{5'(1')}$iminium ion were pooled and further purified on an Oasis MCX Sep-Pac (Waters, Milford, MA). The iminium ion was eluted with methanol containing 2% ammonium hydroxide following the protocol used previously for the isolation of nicotine from plasma (Bloom et al., 2011). The [5-^{3}H]nicotine $\Delta^{5'(1')}$iminium ion was stored at −80°C and used within 10 days of the purification because of instability.

Nicotine $\Delta^{5'(1')}$Iminium Ion Metabolism by CYP2A6 and CYP2A13. The purified P450 enzymes were reconstituted with reductase and lipid as described above. The ratio of P450 to reductase was 1:2. Tris buffer (100 mM, pH 7.4) and catalase (60 units/μl) were added to the reconstituted enzyme to achieve a P450 concentration of 0.5 pmol P450/μl, 1.0 pmol P450/μl, or 2.0 pmol P450/μl. Aliquots of the reconstituted enzyme were added to 100 mM Tris buffer, pH 7.4, NADPH-generating system, and [5-^{3}H]nicotine $\Delta^{5'(1')}$iminium ion (specific activity, 0.02–2.0 Ci/mmol; 5–500 μM) in a final volume of 200 μl. Reactions, carried out at 37°C, were terminated by the addition of either 20 μl of 15% triflouroacetic acid (for analysis using HPLC system I) or 20 μl each of 0.3 M barium hydroxide and zinc

sulfate (for analysis using HPLC system II) and centrifuged at 1500*g* (10 min), and the supernatant was removed and analyzed the same day by one of two HPLC systems (see below).

The metabolites were identified by coelution with standards (UV detection at 254 nm) and LC/MS/MS analysis. The analysis was performed on an Agilent 1100 series capillary HPLC system (Agilent Technologies, Santa Clara, CA) interfaced to a Thermo Scientific TSQ Vantage triple quadrupole mass spectrometer (Thermo Fisher Scientific, Waltham, MA). Samples and standards (4–8 μl) were injected on a 0.5 × 100-mm Zorbax C18 (5-μm particle size) capillary column (Agilent Technologies). The analytes were eluted isocratically with 0.1% TFA in water for 5 min followed by a linear gradient to 30% acetonitrile containing 0.1% TFA over 15 min. The flow rate was 15 μl/min. The unknown peak eluting at 28 min generated by CYP2A6 with either 5 or 100 μM nicotine $\Delta^{5'(1')}$iminium ion was collected from HPLC system II before analysis by LC/MS and LC/MS/MS.

To determine kinetic parameters a series of preliminary experiments were carried out to find conditions that minimized both the inactivation of the enzymes and the secondary metabolism of cotinine. Experiments were performed that varied both time (2.5–30 min for CYP2A13 and 2.5–120 min for CYP2A6) and enzyme concentrations (12.5–60 nM for CYP2A13 and 25–100 nM for CYP2A6). Because of inactivation of the enzymes short reaction times were required to obtain a linear rate of product formation (2.5–5 min for CYP2A13 and 5–20 min for CYP2A6). At high enzyme concentrations significant secondary metabolism occurred. A time course at low enzyme concentrations (2.5–5 pmol for CYP2A13 and 5–10 pmol for CYP2A6) using different nicotine $\Delta^{5'(1')}$iminium ion concentrations was performed to finalize conditions. The conditions that were used to estimate the kinetic parameters were 5, 10, 15, 25, 50, 75, and 100 μM nicotine $\Delta^{5'(1')}$iminium ion with 3 pmol CYP2A13 and 10, 25, 50, 100, 200, and 400 μM with 10 pmol CYP2A6. Reaction times were 4 and 20 min for CYP2A13 and CYP2A6, respectively. Some secondary metabolism still occurred under these conditions. Michaelis-Menten constants were calculated for cotinine formation by using EZ-Fit 5 software (Perrella Scientific, Amherst MA).

Sequential Metabolism of the Nicotine $\Delta^{5'(1')}$Iminium Ion by CYP2A6 and CYP2A13. These experiments were carried out at 30°C to mimic the inactivation experiments. Reconstituted CYP2A13 (25 pmol, at 0.5 pmol P450/μl) was incubated with either 5 μM [5-^{3}H]nicotine $\Delta^{5'(1')}$iminium ion (S.A. = 4 μCi/nmol), 5 μM [^{3}H]cotinine (S.A. = 4 μCi/nmol), or both 5 μM 5-[^{3}H]nicotine $\Delta^{5'(1')}$iminium ion (S.A. = 4 μCi/nmol) and 50 μM cotinine and 1 mM NADPH in 50 mM Tris buffer, pH 7.4. Reconstituted CYP2A6 (25 pmol, at 0.5 pmol P450/μl) was incubated with 5 μM [^{3}H]nicotine $\Delta^{5'(1')}$iminium ion (S.A. = 4 μCi/nmol) and 1 mM NADPH in 50 mM Tris buffer, pH 7.4. Aliquots (12 μl) were removed at 1, 2.5, 5, and 10 min for CYP2A13 or 2.5, 5, 10, and 20 min for CYP2A6, and 1.2 μl each of 0.3 M barium hydroxide and zinc sulfate were added to the aliquot to terminate the reaction. The samples were analyzed by HPLC system II with UV and radioflow detection (β-Ram; IN/US Systems, Tampa, FL). Metabolites were identified by coelution with standards. The identity of the metabolites was confirmed by LC/MS and LC/MS/MS analysis as described above.

To determine the specific activity of the 3′-hydroxycotinine and 5′-hydroxycotinine formed during CYP2A13-mediated [^{3}H]nicotine $\Delta^{5'(1')}$iminium ion metabolism, reconstituted CYP2A13 (25 pmol, at 0.5 pmol P450/μl) was incubated with 5 μM [^{3}H]nicotine $\Delta^{5'(1')}$iminium ion (S.A. = 2 μCi/nmol) in the presence and absence of 10 and 100 μM cotinine for 5 min at 30°C. Three independent experiments were performed for each iminium ion/cotinine combination. For each experiment the *trans*-3′-hydroxycotinine and 5′-hydroxycotinine peaks were collected from HPLC system II, and d_9-*trans*-3′-hydroxycotinine was added as an internal standard to each fraction. The fractions were analyzed by capillary LC/MS/MS (triplicate injections for each) to determine the concentration of 3′-hydroxycotinine or 5′-hydroxycotinine. The method used to analyze 3′-hydroxcotinine in plasma was described previously (Bloom et al., 2011). Standard curves for both 3′-and 5′-hydroxycotinine were determined. The radioactivity present in each was determined by analyzing triplicate aliquots on a Beckman Coulter (Fullerton, CA) LS6500 scintillation counter.

HPLC Systems. In system I, the metabolites were separated on a Luna C_{18} reverse-phase HPLC column (0.46 × 25 cm; 5 μm; Phenomenex, Torrance, CA) and eluted isocratically with 0.2% TFA, pH 1.6 at a flow rate of 0.7 ml/min. In system II, the metabolites were separated on a Gemini C18 column (0.46 × 25 cm; 5 μm; Phenomenex) over 45 min at a flow rate of 1 ml/min. The mobile phase consisted of 20 mM ammonium bicarbonate, pH 9.4 (A) and acetonitrile (B). The metabolites were eluted with a gradient from 4 to 6% B in 20 min, then to 20% B in 5 min, then to 35% B in 5 min, followed by a 10-min hold at 35% B.

Effects of the Nicotine $\Delta^{5'(1')}$Iminium Ion on CYP2A6- and CYP2A13-Mediated Coumarin 7-Hydroxylase Activity. CYP2A6 or CYP2A13 were reconstituted with reductase and lipid as described above. Catalase and Tris buffer were added to the reconstituted enzymes to give final concentrations of 0.5 pmol/μl P450, 1 pmol/μl reductase, 0.1 μg/μl lipid, 35 U/μl catalase, and 50 mM Tris buffer, pH 7.4. To minimize the loss of enzyme activity in the absence of substrate, reactions were carried out at 30°C as described previously for nicotine-mediated inactivation experiments (von Weymarn et al., 2006).

Time-, Concentration-, and NADPH-Dependent Inactivation of CYP2A6 and CYP2A13 by the Nicotine $\Delta^{5'(1')}$Iminium Ion. Nicotine $\Delta^{5'(1')}$iminium ion (0–200 μM) and 1 mM NADPH were added to the reconstituted enzyme solution described above to generate the primary reaction mixture. The primary reaction mixtures were incubated for 5 min at 30°C before the addition of NADPH (1 mM). Upon addition of NADPH, aliquots (5 μl; 2.5 pmol P450) were removed at the indicated times (0–60 min for CYP2A6; 0–30 min for CYP2A13) and added to a secondary reaction mixture (200 μl; a 40-fold dilution) for the determination of coumarin 7-hydroxylation activity remaining as described previously (von Weymarn et al., 1999, 2006). Reactions were carried out at 30°C to minimize the loss of enzyme activity in the absence of substrate as described previously for nicotine inactivation experiments (von Weymarn et al., 2006).

Partition Ratio. CYP2A13 was reconstituted, and the primary reaction mixtures were prepared as described above. Primary reaction mixtures containing 0, 2.5, 5, 10, 20, 40, 80, 160, or 500 μM nicotine $\Delta^{5'(1')}$iminium ion were incubated for 60 min at 30°C in the presence of 1 mM NADPH. Aliquots containing 2.5 pmol of CYP2A13 (5 μl) were removed at 0 and 30 min, and the 7-hydroxycoumarin activity remaining was determined in a secondary reaction mixture as described above. Three independent experiments were performed in duplicate. The partition ratio was determined for each independent experiment, and the values were averaged.

Substrate Protection. Nicotine $\Delta^{5'(1')}$iminium ion inactivation experiments were carried out in the presence of alternate substrates, cotinine and coumarin for CYP2A13 or (*S*)-NNN for CYP2A6. These experiments were carried out as described previously (von Weymarn et al., 2005). CYP2A6 reactions contained 200 μM nicotine $\Delta^{5'(1')}$iminium ion and were incubated for 60 min. CYP2A13 reactions were incubated with 50 μM nicotine $\Delta^{5'(1')}$iminium ion for 30 min. The concentrations of (*S*)-NNN in the CYP2A6 primary reactions were 0, 10, or 50 μM. In the CYP2A13 reactions, the concentrations of the alternate substrates were 0, 50, or 400 μM for cotinine and 50 μM for coumarin. The control sample did not contain either the iminium ion or the alternate substrate. When coumarin was used as an alternate substrate additional control reactions were carried out. These controls, in which no coumarin was added to the secondary reaction, were used to quantify the 7-hydroxycoumarin formed in the primary reactions that was transferred into the secondary reaction. To calculate the CYP2A13 activity in the secondary reaction the amount of 7-hydroxycoumarin formed in the controls was subtracted from that formed in the complete secondary reactions.

Irreversibility of Inactivation. The irreversibility experiments were performed as described previously (von Weymarn et al., 2005). Reconstituted CYP2A6 and CYP2A13 was incubated with the nicotine $\Delta^{5'(1')}$iminium ion (50 μM for CYP2A13; 100 μM for CYP2A6) in the presence (inactive) or absence (control) of 1 mM NADPH in 50 mM Tris buffer, pH 7.4. Samples were incubated 5 min without NADPH at 30°C. At 0 and 20 min (CYP2A13) or 30 min (CYP2A6) after NADPH addition the samples were analyzed for coumarin 7-hydroxylation activity remaining, spectrally active protein, by reduced CO spectra remaining and the amount of native heme as determined by HPLC with UV detection. The remainder of the control and inactivated samples (200–250 μl) was applied to a G50 Sephadex spin column (von Weymarn et al., 2004); samples were then reconstituted with lipid and analyzed for coumarin 7-hydroxylation activity, the formation of a reduced CO spectrum, and native heme.

Results

The nicotine $\Delta^{5'(1')}$iminium ion was an inactivator of both CYP2A6 and CYP2A13 (Fig. 2). The inactivation was linear with time and did not occur in the absence of NADPH. It was difficult to find a range of iminium ion concentrations that resulted in a linear loss of CYP2A6 activity (Fig. 2A). At concentrations below 50 μM inactivation was not detected, and at concentrations above 100 μM the extent of inactivation did not increase. Despite the lack of linearity with nicotine $\Delta^{5'(1')}$iminium ion concentration the kinetic parameters for the inactivation of CYP2A6 by the iminium ion were estimated from the double-reciprocal plot of 1/k versus 1/[iminium ion]. The estimated K_i for the inactivation of CYP2A6 was 300 μM, the k_{inact} was 0.03 min^{-1}, and the $t_{1/2}$ was 27 min. The inactivation of CYP2A13 by the nicotine $\Delta^{5'(1')}$iminium ion was linear over a range of concentrations (Fig. 2B) and was more efficient than inactivation of CYP2A6; the K_i was 30 μM and the k_{inact} was 0.04 min^{-1} with a $t_{1/2}$ of 15.5 min.

The partition ratio, the number of molecules of the inactivator metabolized per molecule of enzyme inactivated, was determined by allowing the inactivation to go to completion at varying iminium ion concentrations (Fig. 3). In the case of CYP2A13 maximum inactivation resulted in the loss of 80% of the enzyme's activity, and the partition ratio was 42 ± 7 (mean ± S.D.; n = 3). It was not possible to quantify the partition ratio for CYP2A6, because significant coumarin 7-hydroxylation activity was lost when CYP2A6 was incubated with NADPH for the 60 min required for complete inactivation by the nicotine $\Delta^{5'(1')}$iminium.

Both CYP2A6 and CYP2A13 were protected from nicotine $\Delta^{5'(1')}$iminium ion-mediated inactivation by the addition of alternate substrates (Table 1). The addition of (*S*)-NNN, an excellent substrate for CYP2A6 (K_m, 2.3 μM; V_{max}, 1.0 min^{-1}) (Wong et al., 2005) resulted in complete protection. However, cotinine (K_m, 61 μM; V_{max}, 11 min^{-1}) (Brown et al., 2005) present at 400 μM provided only modest protection of CYP2A13. Therefore, coumarin, which is an excellent substrate for CYP2A13 (K_m <1 μM) (von Weymarn and Murphy, 2003), was used as an alternate substrate. In the presence of 50 μM coumarin CYP2A13 was completely protected from nicotine $^{\Delta 5'(1')}$iminium ion-mediated inactivation.

The irreversibility of nicotine $\Delta^{5'(1')}$iminium ion-mediated inactivation was confirmed for both CYP2A6 and CYP2A13. Under conditions in which the inactivation of CYP2A13 by 50 μM nicotine $\Delta^{5'(1')}$iminium ion resulted in a 50 ± 3% loss in coumarin 7-hydroxylation activity, a 16 ± 2.5% loss in intact heme and 55 to 70% loss in reduced CO spectra were ob-

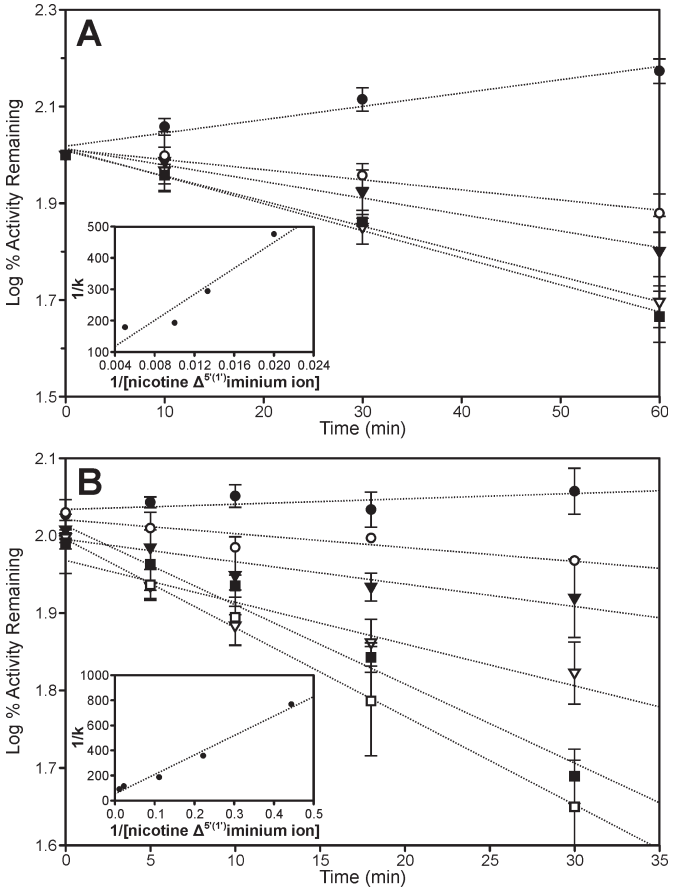

Fig. 2. Time- and concentration-dependent inactivation of CYP2A6 (A) and CYP2A13 (B) by the nicotine $\Delta^{5'(1')}$iminium ion. Activity remaining refers to coumarin 7-hydroxylation activity measured in a secondary reaction at the indicated times. The $\Delta^{5'(1')}$iminium ion concentrations are 0 (●), 50 (○), 75 (▼), 100 (△), and 200 (■) μM for CYP2A6 and 0 (●), 5 (○), 10 (▼), 25 (△), 50 (■), and 100 (□) μM for CYP2A13. Values are mean ± S.D. from three independent experiments performed in duplicate. The insets represent the double-reciprocal plot generated from the slopes of the lines at the various concentrations.

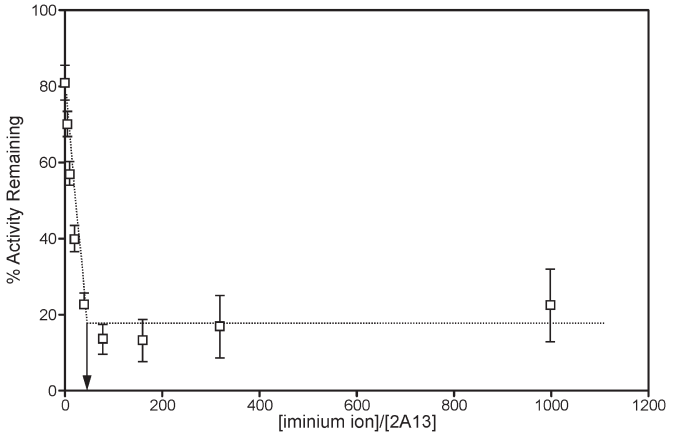

Fig. 3. Partition ratio determination for CYP2A13 with the nicotine $\Delta^{5'(1')}$iminium ion. The inactivation was allowed to go to completion, then coumarin 7-hydroxylation activity was determined in a secondary reaction. Values are the means ± S.D. of three independent experiments preformed in duplicate. The arrow indicates the intercept used to determine the partition ratio.

TABLE 1

Effects of alternate substrates on nicotine $\Delta^{5'(1')}$iminium ion-mediated inactivation of CYP2A6 and CYP2A13

Enzymes were incubated with nicotine $\Delta^{5'(1')}$iminium ion (200 μM for 60 min with CYP2A6; 50 μM for 20 min with CYP2A13) at 30°C, in the presence of alternate substrate. Coumarin 7-hydroxylation activity was determined in a secondary reaction as described under *Materials and Methods*. The values reported are the mean ± S.D. for three independent experiments.

	Alternate Substrate	Ratio of Iminium Ion/ Alternate Substrate	Percentage Activity Remaining
CYP2A6		1:0	46 ± 7
CYP2A6	NNN, 10 μM	20:1	50 ± 3
CYP2A6	NNN, 50 μM	4:1	111 ± 13
CYP2A13		1:0	38 ± 1
CYP2A13	Cotinine, 50 μM	1:1	48 ± 4
CYP2A13	Cotinine, 400 μM	1:8	69 ± 2

served. These values were not altered by spin-column gel filtration. The data for CYP2A6 and 100 μM iminium ion were similar: 50 ± 1.5% activity loss, 27 ± 8% loss of intact heme; and 65% loss in spectrally active protein.

The addition of exogenous nucleophiles to an inactivation reaction is often used to characterize a compound as a true mechanism-based inactivator, that is, a compound that upon metabolism covalently modifies the active site of the enzyme. However, protection by exogenous nucleophiles, such as glutathione and cyanide, could not be assessed with the nicotine $\Delta^{5'(1')}$iminium ion, because it will react with the nucleophile before being metabolized. The nicotine $\Delta^{5'(1')}$iminium ion has been shown to covalently modify proteins (Shigenaga et al., 1988), but it did not inactivate either CYP2A6 or CYP2A13 in the absence of NADPH.

To gain a better understanding of the mechanism of CYP2A6 and CYP2A13 inactivation by the nicotine $\Delta^{5'(1')}$iminium ion, its metabolism was studied in detail. The metabolites generated were characterized by coelution with standards in two HPLC systems (Figs. 4 and 5), and their identity was confirmed by LC/MS and LC/MS/MS analysis. The primary product generated by both enzymes was cotinine. No aldehyde oxidase was present in the reaction mixture, and cotinine formation depended on the presence of NADPH.

The cotinine metabolite, *trans*-3′-hydroxycotinine was detected within 5 min of cotinine formation by CYP2A13 (Fig. 4A). The concentration of cotinine was <0.5 μM at this time, significantly below the K_m of CYP2A13-catalyzed cotinine 3′-hydroxylation (61 μM). At 20 min, additional cotinine metabolites were detected as secondary metabolites of the nicotine $\Delta^{5'(1')}$iminium (Fig. 4B). To further characterize these metabolites, experiments were carried out with increased enzyme and decreased nicotine $\Delta^{5'(1')}$iminium concentrations. The products of these reactions were analyzed with a second HPLC system (Fig. 5), which allowed separation of the *cis* and *trans* isomers of 3′-hydroxycotinine. To maximize product formation excess enzyme was used to generate the data presented in Fig. 5. Both *cis* and *trans* 3′-hydroxycotinine were products of CYP2A13-catalyzed nicotine $\Delta^{5'(1')}$iminium metabolism, and both increased with time (Fig. 5, A and B). 5′-Hydroxycotinine, norcotinine, and *N*-hydroxymethylnorcotinine were also identified as products. The identity and relative amounts of norcotinine and 5′-hydroxycotinine were confirmed by collection from HPLC system II and analysis on HPLC system I.

Cotinine and cotinine metabolites were also detected as products of CYP2A6-catalyzed nicotine $\Delta^{5'(1')}$iminium metab-

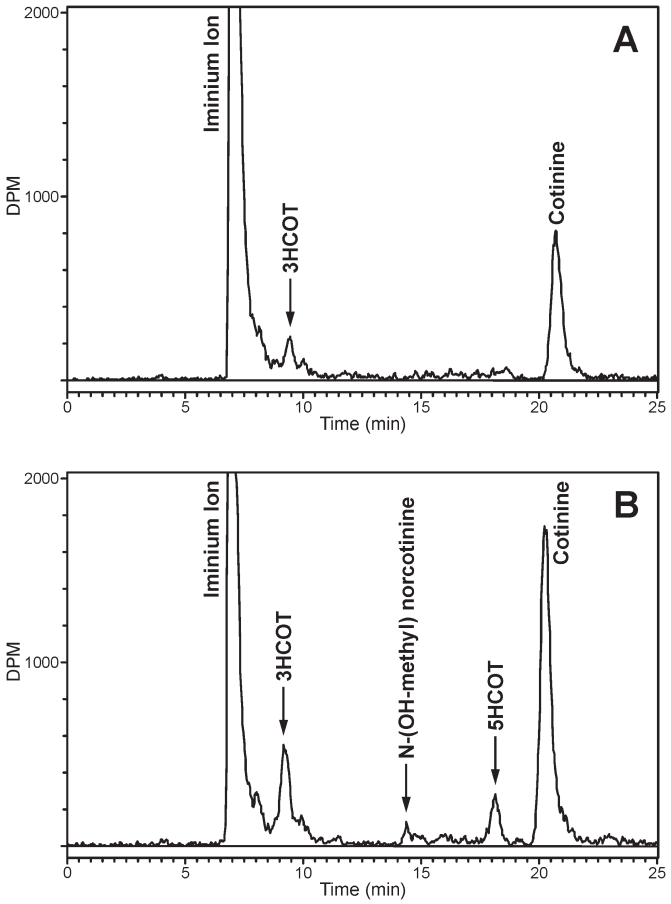

Fig. 4. Radioflow HPLC analysis of CYP2A13-mediated metabolism of nicotine $\Delta^{5'(1')}$iminium ion on system I. CYP2A13 (3 pmol) was incubated with 20 μM [5-^{3}H]nicotine $\Delta^{5'(1')}$iminium ion (specific activity, 0.1 μCi/nmol) for 5 min (A) or 20 min (B). The retention times were confirmed by coelution with standards in each sample.

olism (Fig. 5, C and D). The metabolites identified were *cis*- and *trans*-3′-hydroxycotinine and the products of methyl oxidation, *N*-(hydroxymethyl)norcotinine and norcotinine. 5′-Hydroxycotinine was not detected. The radioactive peak at 28 min did not coelute with any available standard and was a product of both CYP2A6- and CYP2A13-catalyzed metabolism of the nicotine $\Delta^{5'(1')}$iminium. This peak was collected and analyzed by LC/MS/MS. The parent ion detected was *m/z* 177 (M+H). The product ion spectra of this metabolite contained three primary fragments, *m/z* 118 (100%), *m/z* 159 (60%), and *m/z* 80 (48%). The *m/z* 159 fragment was proposed to be protonated β-nicotyrine generated by the loss of water, consistent with the presence of a hydroxyl group and a double bond in the pyrrolidine ring of the parent ion. The major fragment, *m/z* 118, a common fragment of nicotine-related compounds (Hecht et al., 1981; Tuomi et al., 1999), contains the pyridine ring and three carbons of the pyrrolidine ring, and *m/z* 80 is the pyridinium ion. These fragmentation data support the tentative identification of this metabolite as 2′-hydroxy-3′,4′-dehydronicotine or a related isomer.

The kinetic parameters for the formation of cotinine from the nicotine $\Delta^{5'(1')}$iminium were estimated under conditions that minimized inactivation and the formation of secondary metabolites. CYP2A13 was a more efficient catalyst of this reaction than was CYP2A6. The apparent K_m for CYP2A13-

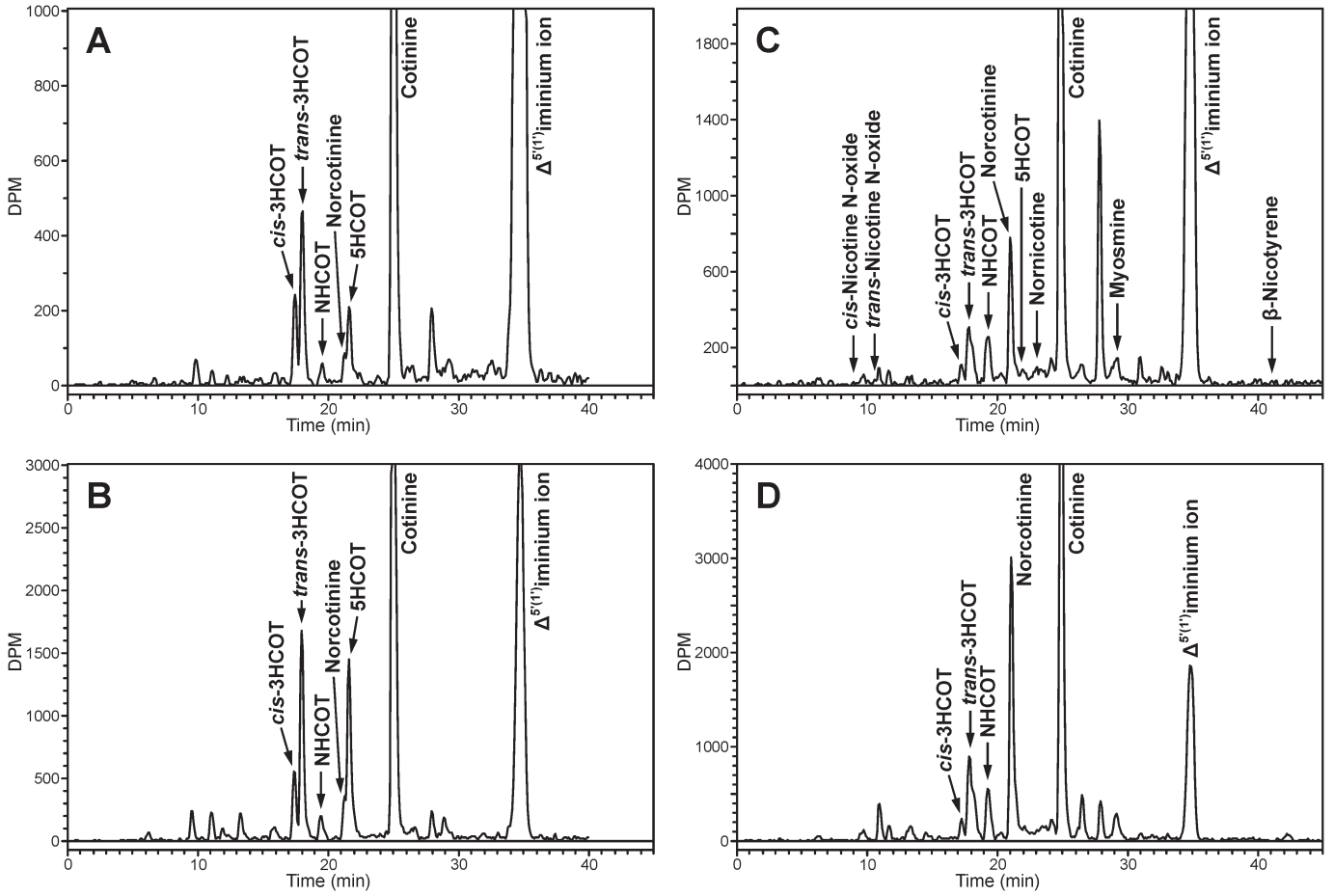

Fig. 5. Radioflow HPLC analysis of nicotine $\Delta^{5'(1')}$iminium ion metabolism by CYP2A6 and CYP2A13 on system II. [5-^{3}H]nicotine $\Delta^{5'(1')}$iminium ion (5 μM; 4 μCi/nmol) was incubated with CYP2A13 (25 pmol) for 5 min (A) and 20 min (B) or with CYP2A6 (25 pmol; 4 μCi/nmol) for 5 min (C) and 10 min (D). Retention times were confirmed by coelution with standards. A mix of standards, which included *cis*-3HCOT (r_t = 17.3 min), *trans*-3HCOT (r_t = 18.0 min), NHCOT (r_t = 19.2 min), norcotinine (r_t = 21.1 min), 5HCOT (r_t = 21.7 min), nornicotine (r_t = 23.0 min), and cotinine (r_t = 25.1 min), was added to each sample. *cis*-Nicotine *N*-oxide (r_t = 9.1 min), *trans*-nicotine *N*-oxide (r_t = 10.2 min), myosmine (r_t = 29.2 min), and β-nicotyrine (r_t = 41.1 min) were added to a subset of samples.

TABLE 2

CYP2A13-catalyzed [^{3}H]cotinine and [^{3}H]nicotine $\Delta^{5'(1')}$iminium ion metabolism

CYP2A13 (25 pmol) was incubated with the indicated substrates (4 μCi/nmol) at 30°C. Aliquots were removed from each sample at the indicated times and analyzed on HPLC system II. The values are the mean ± S.D. for four independent experiments.

Substrate (5 μM)	Time	Ratio of Products		Percentage Total Radioactivity Cotinine
		cis-3HCOT/*trans*-3HCOT	3HCOT[a]/ 5HCOT	
	min			
[^{3}H]nicotine $\Delta^{5'(1')}$iminium ion	1	0.5 ± 0.08[b]	4.5 ± 0.3[b]	15 ± 3
	2.5	0.4 ± 0.05	2.6 ± 0.3	25 ± 3
	5	0.4 ± 0.02	1.9 ± 0.2	37 ± 4
	10	0.3 ± 0.02[b]	1.1 ± 0.1[b]	47 ± 3
[^{3}H]cotinine	1	No *cis*-3HCOT	N.D.	N.D.
	2.5	No *cis*-3HCOT	0.2 ± 0.1	93 ± 3
	5	No *cis*-3HCOT	0.3 ± 0.1	94 ± 2
	10	No *cis*-3HCOT	0.2 ± 0.1	94 ± 1

N.D., not detected.
[a] *cis* and *trans* isomers combined.
[b] Values significantly different by paired one-tailed t-test; $P < 0.005$

mediated $\Delta^{5'(1')}$iminium ion metabolism was 28 ± 4 μM, and the V_{max} was 12.9 ± 0.7 nmol/min/nmol, whereas the apparent K_m and V_{max} values for CYP2A6 were 229 ± 49 μM and 6.0 ± 0.7 nmol/min/nmol, respectively.

The product distribution of the secondary metabolites formed from the nicotine $\Delta^{5'(1')}$iminium ion varied with time and differed significantly between the two enzymes. *trans*-3′-Hydroxycotinine was the major secondary metabolite generated by CYP2A13 (Fig. 5, A and B). The *cis* isomer was also detected; however, as the reaction time was increased the ratio of the *cis* to *trans* isomer decreased (Table 2). In addition, the amount of 5′-hydroxycotinine relative to both *cis*- and *trans*-3′-hydroxycotinine increased with longer reaction times (Table 2). 5′-Hydroxycotinine was not detected as a

TABLE 3

CYP2A6-catalyzed [^{3}H]nicotine $\Delta^{5'(1')}$iminium ion metabolism

CYP2A6 (25 pmol) was incubated with 5 μM(4 μCi/nmol) [^{3}H]nicotine $\Delta^{5'(1')}$iminium ion at 30°C. At the indicated times aliquots were analyzed on HPLC system II as described under *Materials and Methods*. The values reported are the mean ± S.D. for four independent experiments.

Time	Percentage of Radioactivity[a]				Ratio	
	Iminium Ion	Cotinine	NCOT and NHCOT[b]	3HCOT[c]	*cis*-3HCOT/*trans*-3HCOT	3HCOT[c]/NCOT and NHCOT
2.5 min	85 ± 5	4 ± 1	2 ± 0.5	2 ± 1	0.4 ± 0.2	1.0 ± 0.4
5 min	77 ± 3	7 ± 2	5 ± 1	3 ± 1	0.3 ± 0.04	0.6 ± 0.2
10 min	64 ± 3	11 ± 2	10 ± 2	4 ± 1	0.3 ± 0.2	0.5 ± 0.2
20 min	50 ± 6	15 ± 1	19 ± 2	6 ± 2	0.2 ± 0.1	0.3 ± 0.1

[a] Percentage of the sum of all metabolites and the nicotine $\Delta^{5'(1')}$iminium ion quantified by HPLC.
[b] Sum of NHCOT and NCOT.
[c] Sum of *cis*- and *trans*-isomers 3HCOT.

product of CYP2A6-catalyzed metabolism (Fig. 5, C and D). Norcotinine and 3′-hydroxycotinine both were detected as secondary metabolites. The formation of norcotinine increased significantly with time relative to the formation of 3′-hydroxycotinine (Table 3). At 2.5 min the products of cotinine methylhydroxylation were present in a 1:1 ratio with 3′-hydroxycotinine; by 20 min this ratio had decreased to 0.3 (Table 3). Both *cis*- and *trans*-3′-hydroxycotinine were detected and, as with CYP2A13, the ratio of the *cis* to *trans* isomer decreased with time.

The secondary metabolites of the nicotine $\Delta^{5'(1')}$iminium were presumed to be the products of cotinine metabolism. However, we reported previously that 5′-hydroxycotinine was a product of CYP2A6-catalyzed cotinine metabolism and it was the major product of CYP2A13-catalyzed cotinine metabolism (Murphy et al., 1999; Brown et al., 2005). We repeated the analysis of cotinine metabolism by these two enzymes under the same conditions as those used for the metabolism of the nicotine $\Delta^{5'(1')}$iminium ion (Fig. 5). As reported previously (Murphy et al., 1999; Brown et al., 2005), 5′-hydroxycotinine was detected as a metabolite of CYP2A6-catalyzed cotinine metabolism (data not shown) and was the major product of CYP2A13-catalyzed cotinine metabolism. In Table 2, the ratio of 3′-hydroxycotinine to 5′-hydroxycotinine generated by CYP2A13-catalyzed metabolism of cotinine and the nicotine $\Delta^{5'(1')}$iminium ion are compared. When the substrate was cotinine, no *cis*-3′-hydroxycotinine was detected, and the ratio of 3′-hydroxy to 5′-hydroxycotinine was 0.2 to 0.3 at all reaction times. In contrast, when the substrate was the nicotine $\Delta^{5'(1')}$iminium ion the ratio of 3′-hydroxy to 5′-hydroxycotinine decreased with time as the concentration of cotinine increased (Fig. 5, A and B; Table 2). After 1 min when 15% of the radioactivity was present as cotinine the ratio of 3′-hydroxy to 5′-hydroxycotinine was 4.5 ± 0.3. After 10 min when cotinine accounted for 47% of the radioactivity (a concentration of 2.5 μM), the ratio decreased to 1.1 ± 0.1. The observed change in the ratio of 3′-hydroxy to 5′-hydroxycotinine was the result of an increased rate of 5′-hydroxycotinine formation (Table 4). Because of the mechanism-based inactivation of the enzyme, the rate of formation of the sum of all major metabolites decreased significantly from the first to the 10th minute of the reaction. However, the rate of 5′-hydroxycotinine formation increased over this time period, and the rate of total 3′-hydroxycotinine formation decreased (Table 4). These data and the fact that CYP2A13 catalyzes the 5′-hydroxylation of cotinine at a rate five times the rate of 3′ hydroxylation led us to assume that the increased rate of formation of 5′-hydroxycotinine was caused by the metabolite cotinine re-entering the active site as a substrate. 3′-Hydroxycotinine may be formed primarily as a product of the sequential metabolism of the nicotine $\Delta^{5'(1')}$iminium ion, that is two oxidation reactions occur before product release from the enzyme.

TABLE 4

Rate of tritiated product formation during CYP2A13-mediated [^{3}H]nicotine $\Delta^{5'(1')}$iminium ion metabolism in the absence and presence of cotinine

CYP2A13 (25 pmol,) was incubated with 5 μM (4 μCi/nmol) [^{3}H]nicotine $\Delta^{5'(1')}$iminium ion in the absence of presence of 50 μM cotinine at 30°C. Aliquots were taken at the indicated times and analyzed on HPLC system II with radioflow detection. Values are calculated using the specific activity of the iminium ion, means ± S.D. for four independent experiments.

Addition	Time	Rate of Formation, pmol/min/pmol CYP2A13		
		Total [^{3}H] Metabolites[a]	[^{3}H]3HCOT[b]	[^{3}H]5HCOT
	min			
None	1	0.32 ± 0.03[c]	0.23 ± 0.04	0.05 ± 0.01
	10	0.24 ± 0.03[c]	0.12 ± 0.02	0.12 ± 0.02[d]
Cotinine, 50 μM	1	0.24 ± 0.02[c]	0.18 ± 0.02	0.05 ± 0.01
	10	0.19 ± 0.01[c]	0.10 ± 0.01	0.08 ± 0.01[d]

[a] Includes cotinine, *cis*- and *trans*-3HCOT, 5HCOT), norcotinine, *N*-(hydroxymethyl)norcotinine, and the 28-min peak.
[b] Sum of *cis* and *trans* isomers.
[c] Values are significantly different by *t* test; $P < 0.02$.
[d] Values are significantly different by *t* test; $P < 0.005$.

To further investigate the possible CYP2A13-catalyzed sequential metabolism of the nicotine $\Delta^{5'(1')}$iminium ion to cotinine and then to 3′-hydroxycotinine, the metabolism of [5-^{3}H]nicotine $\Delta^{5'(1')}$iminium ion was carried out in the presence and absence of nonradioactive cotinine. The nonradioactive cotinine should compete with the oxidation of [^{3}H]cotinine released for the active site, but should not affect sequential metabolism. The rates of [5-^{3}H]3′-hydroxycotinine to [5-^{3}H]5′-hydroxycotinine formation in the presence and absence of cotinine are compared in Table 4. The rate of total [^{3}H]metabolite formation was slower at 1 and 10 min in the presence of cotinine. The decrease was modest given the approximately 25-fold ratio of nonradioactive to radioactive cotinine. This may in part be explained by protection of the enzyme from inactivation resulting in an overall increase in enzyme activity. However, the rate of [^{3}H]3′-hydroxycotinine formation at 10 min was not significantly affected by the presence of unlabeled cotinine. In the presence of unlabeled cotinine the rate of [^{3}H]5′-hydroxycotintine formation decreased 30%, from 0.12 to 0.08 pmol/min/pmol CYP2A13. These data are consistent with the hypothesis that the formation of [^{3}H]5′-hydroxycotinine is caused by the metabolism of [^{3}H]cotinine that re-enters the active site of the enzyme and that the [^{3}H]3′-hydroxycotinine formation may occur by sequential metabolism of the [^{3}H]nicotine-$\Delta^{5'(1')}$iminium ion.

To confirm the differential effect of nonradioactive cotinine on the formation of tritiated 3′- and 5′-hydroxycotinine from the [^{3}H]nicotine $\Delta^{5'(1')}$iminium ion (5 μM), the specific activity of these two metabolites was determined after a 5-min reaction. In this experiment, the concentration of cotinine was 100 μM. Aliquots of the tritiated products were isolated by using HPLC system II, the radioactivity present was quantified by scintillation counting, and the concentration of the metabolite was determined by LC/MS/MS. The specific activity of 5′-hydroxycotinine was 4.0 μCi/nmol in the absence of cotinine and 0.24 μCi/nmol in the presence of cotinine. The specific activity of 3′-hydroxycotinine was 4.0 μCi/nmol when unlabeled cotinine was not added and 0.54 μCi/nmol when it was added. These data are consistent with a portion of the 3-hydroxycotinine being formed from the oxidation of [^{3}H]cotinine that is not diluted with unlabeled cotinine. We were unable to independently calculate the specific activity of the *cis* and *trans* isomers of 3′-hydroxycotinine because of the 30-s separation between the tritiated and nontritiated metabolites and the small separation between the *cis* and *trans* isomers obtained by HPLC.

Discussion

We reported previously that both CYP2A6 and CYP2A13 were inactivated during nicotine metabolism (von Weymarn et al., 2006). However, the inactivation occurred after nicotine metabolism was complete. This led us to suggest that oxidation of a nicotine metabolite, possibly the nicotine $\Delta^{5'(1')}$iminium ion, was responsible for generating the inactivating species. In the studies presented here we confirm that the nicotine $\Delta^{5'(1')}$iminium ion is an inactivator of both CYP2A6 and CYP2A13, and that inactivation depends on time, concentration, and the presence of NADPH. Inactivation was not reversible, the presence of alternate substrates protected both enzymes from inactivation, and the observed loss in enzyme activity was accompanied by a parallel loss in spectrally active protein, as measured by reduced CO spectrum. These data all are consistent with the characterization of the nicotine $\Delta^{5'(1')}$iminium ion as a mechanism-based inactivator of both CYP2A13 and CYP2A6.

Denton et al. (2004) reported that the nicotine $\Delta^{5'(1')}$iminium ion was a poor inhibitor of CYP2A6 ($K_i \geq 300$ μM) and then concluded that "a species on the reaction path before the iminium ion is responsible for nicotine-mediated inhibition" of CYP2A6. We report an estimated K_i for the inactivation of CYP2A6 by the nicotine $\Delta^{5'(1')}$iminium ion of 300 μM and have concluded that the nicotine metabolite responsible for inactivation of CYP2A6 is a metabolite of the iminium ion. This conclusion is supported by our earlier report (von Weymarn et al., 2006) that nicotine-mediated inactivation of CYP2A6 and CYP2A13 occurred as secondary and tertiary metabolism of nicotine were detected and now by our characterization of the iminium ion as a mechanism-based inactivator of both CYP2A6 and CYP2A13.

The relatively high K_i for nicotine $\Delta^{5'(1')}$iminium ion-mediated inactivation may not be an accurate measure of its potency as an inactivator if, when it forms as the primary product of nicotine metabolism, a portion is further oxidized before release from the active site of the enzyme. This would require that CYP2A6 catalyzes the sequential metabolism of nicotine. The rapid appearance of cotinine as a metabolite of both CYP2A6- and CYP2A13-catalyzed nicotine metabolism has led us to suggest that this is true (von Weymarn et al., 2006). Sequential metabolism by CYP2A6 has been demonstrated for the oxidation of *N,N*-dimethylnitosamine and *N,N*-diethylnitosamine to formic acid and acetic acid, respectively (Chowdhury et al., 2010). In the study presented here, we confirmed that CYP2A13 catalyzes the sequential metabolism of the nicotine $\Delta^{5'(1')}$iminium ion to 3′-hydroxycotinine. The high K_m of CYP2A6-catalyzed metabolism of the nicotine $\Delta^{5'(1')}$iminium ion made it difficult to characterize secondary metabolism by CYP2A6, but the data obtained support the sequential metabolism of the iminium ion to 3′-hydroxycotinine.

The metabolism of nicotine to cotinine requires two oxidations, and it has been generally accepted that a cytosolic enzyme, aldehyde oxidase, is necessary for the oxidation of the nicotine $\Delta^{5'(1')}$iminium ion to cotinine (Hukkanen et al., 2005). However, rabbit and human liver microsomes have been shown to catalyze the metabolism of nicotine to cotinine with no added cytosol (Shigenaga et al., 1988; Dicke et al., 2005). In addition, both cotinine and the iminium ion were products of CYP2A6- and CYP2A13-catalyzed nicotine metabolism (Murphy et al., 2005; von Weymarn et al., 2006). Cotinine was the primary product of nicotine $\Delta^{5'(1')}$iminium ion metabolism by these enzymes (Fig. 4). Therefore, aldehyde oxidase is not required to metabolize nicotine to cotinine.

During either CYP2A6- or CYP2A13-catalyzed metabolism of the iminium ion secondary metabolites products of cotinine oxidation rapidly appeared (Figs. 4 and 5). It is noteworthy that the distribution of the cotinine metabolites generated by these enzymes from the iminium ion was different from the distribution obtained when the substrate was cotinine (Murphy et al., 1999; Brown et al., 2005). CYP2A13-catalyzed cotinine metabolism generated three to five times more 5′-hydroxycotinine than 3′-hydroxycotinine. In contrast, 3′-hydroxycotinine was initially the primary cotinine metabolite formed during CYP2A13-catalyzed metabolism of the iminium ion. However, as the reaction proceeded the ratio of 3′-hydroxycotinine to 5′-hydroxycotinine decreased significantly. We hypothesized that a portion of the 3′-hydroxycotinine formed was caused by sequential metabolism of the iminium ion and 5′-hydroxcotinine was formed from cotinine released by the enzyme that re-entered the active site in a different orientation. We obtained three pieces of data that supported this hypothesis. One, the rate of 5′-hydroxycotinine formation increased with reaction time, whereas the rate of 3′-hydroxycotine formation decreased (Table 4). Two, the addition of unlabeled cotinine to a CYP2A13 reaction with [^{3}H]iminium ion inhibited the rate of [^{3}H] 5′-hydroxycotinine formation but not the rate of [^{3}H]3′-hydroxycotinine formation (Table 4). Three, the specific activity of the 3′-hydroxycotinine formed was twice that of the 5′-hydroxcotinine when the [^{3}H]iminium ion was metabolized in the presence of unlabeled cotinine.

The primary pathway of CYP2A6-catalyzed cotinine metabolims in vitro was N-hydroxylation (Brown et al., 2005). Deformylation of the product of this pathway, *N*-(hydroxymethyl)norcotinine, generates norcotinine (Fig. 1). Both *N*-(hydroxymethyl)norcotinine and norcotinine were products of CYP2A6-catalyzed nicotine $\Delta^{5'(1')}$iminium ion metabolism, and their formation relative to the formation of 3′-hydroxycotinine increased significantly with time. This is analogous to the observed increased rate of cotinine 5′-

hydroxylation relative to 3′-hydroxylation by CYP2A13-catalyzed iminium ion metabolism. Taken together, these data support the hypothesis that the formation of 3′-hydroxycotinine as a product of CYP2A6-catalyzed metabolism of the nicotine $\Delta^{5'(1')}$iminium ion occurred by sequential metabolism, whereas at least a portion of the norcotinine formed was caused by metabolism of cotinine that re-enters the active site of the enzyme. The relatively high K_m of cotinine metabolism by CYP2A6 (>500 μM) and the fact that 5′-hydroxycotinine, a more abundant metabolite of CYP2A6-catalyzed cotinine metabolism than 3′-hydroxycotinine, was not detected as a product of iminium metabolism, suggest that sequential metabolism may be the dominant pathway.

Although cotinine was the primary product of CYP2A6- and CYP2A13-catalyzed nicotine $\Delta^{5'(1')}$iminium ion metabolism, another product was identified, the "28-min" peak (Fig. 4). This metabolite had the same molecular mass as cotinine but a very different product ion spectra; we have tentatively identified it as 2′-hydroxy-3′,4′-dehydronicotine or a related isomer that would dehydrate to generate β-nicotyrine. β-Nicotyrine has been identified as a metabolite of nicotine in the rat and dog (Werle and Meyer, 1950) and as a product of CYP2A6-catalyzed nicotine metabolism (V. M. Kramlinger and S. E. Murphy, unpublished data). We have recently confirmed that, as suggested by Denton et al. (2004), β-nicotyrine is a mechanism-based inactivator of CYP2A6 (Kramlinger et al., 2012). Therefore, we hypothesize that β-nicotyrine may be a key intermediate in the inactivation of CYP2A6 and CYP2A13 by both nicotine and nicotine $\Delta^{5'(1')}$iminium ion. Experiments are ongoing to test this hypothesis. A second hypothesis to be tested is that nicotine may be metabolized by two sequential oxidations to β-nicotyrine without the iminium ion leaving the active site.

In summary, we report here that the nicotine $\Delta^{5'(1')}$iminium ion is a mechanism-based inactivator of CYP2A6 and CYP2A13, and both enzymes catalyze the metabolism of the nicotine $\Delta^{5'(1')}$iminium ion to cotinine. We also present evidence that CYP2A6 and CYP2A13 catalyze the sequential metabolism of the nicotine $\Delta^{5'(1')}$iminium ion. That is, a fraction of the cotinine formed may not be released from the enzyme before further oxidation to 3′-hydroxycotinine.

Acknowledgments

We thank Katherine Brown for the analysis of the kinetic parameters of CYP2A6- and CYP2A13-catalyzed nicotine $\Delta^{5'(1')}$iminium ion metabolism.

Authorship Contributions

Participated in research design: von Weymarn and Murphy.

Conducted experiments: von Weymarn and Retzlaff.

Performed data analysis: von Weymarn and Murphy.

Wrote or contributed to the writing of the manuscript: von Weymarn and Murphy.

References

Bao Z, He XY, Ding X, Prabhu S, and Hong JY (2005) Metabolism of nicotine and cotinine by human cytochrome P450 2A13. *Drug Metab Dispos* **33:**258–261.

Bloom J, Hinrichs AL, Wang JC, von Weymarn LB, Kharasch ED, Bierut LJ, Goate A, and Murphy SE (2011) The contribution of common CYP2A6 alleles to variation in nicotine metabolism among European-Americans. *Pharmacogenet Genomics* **21:**403–416.

Brandänge S and Lindblom L (1979) The enzyme "aldehyde oxidase" is an iminium oxidase. Reaction with nicotine Δ1′(5′) iminium ion. *Biochem Biophys Res Commun* **91:**991–996.

Brown KM, von Weymarn LB, and Murphy SE (2005) Identification of *N*-(hydroxymethyl) norcotinine as a major product of cytochrome P450 2A6, but not cytochrome P450 2A13-catalyzed cotinine metabolism. *Chem Res Toxicol* **18:**1792–1798.

Chowdhury G, Calcutt MW, and Guengerich FP (2010) Oxidation of *N*-nitrosoalkylamines by human cytochrome P450 2A6: sequential oxidation to aldehydes and carboxylic acids and analysis of reaction steps. *J Biol Chem* **285:**8031–8044.

Denton TT, Zhang X, and Cashman JR (2004) Nicotine-related alkaloids and metabolites as inhibitors of human cytochrome P-450 2A6. *Biochem Pharmacol* **67:** 751–756.

Dicke KE, Skrlin SM, and Murphy SE (2005) Nicotine and 4-(methylnitrosamino)-1-(3-pyridyl)-butanone metabolism by cytochrome P450 2B6. *Drug Metab Dispos* **33:**1760–1764.

Gorrod JW and Hibberd AR (1982) The metabolism of nicotine-Δ1′(5′)-iminium ion, in vivo and in vitro. *Eur J Drug Metab Pharmacokinet* **7**:293–298.

Hanna IH, Teiber JF, Kokones KL, and Hollenberg PF (1998) Role of the alanine at position 363 of cytochrome P450 2B2 in influencing the NADPH- and hydroperoxide-supported activities. *Arch Biochem Biophys* **350:**324–332.

Hecht SS, Chen CB, Young R, and Hoffmann D (1981) Mass spectra of tobacco alkaloid-derived nitrosamines, their metabolites, and related compounds. *Beiträge Tabakforschung* **11:**57–66.

Hukkanen J, Jacob P 3rd, and Benowitz NL (2005) Metabolism and disposition kinetics of nicotine. *Pharmacol Rev* **57:**79–115.

Jalas JR, Hecht SS, and Murphy SE (2005) Cytochrome P450 enzymes as catalysts of metabolism of 4-(methylnitrosamino)-1-(3-pyridyl)-1-butanone, a tobacco-specific carcinogen. *Chem Res Toxicol* **18:**95–110.

Kent UM, Yanev S, and Hollenberg PF (1999) Mechanism-based inactivation of cytochromes P450 2B1 and P450 2B6 by *n*-propylxanthate. *Chem Res Toxicol* **12:**317–322.

Kramlinger VM, von Weymarn LB, and Murphy SE (2012) Inhibition and inactivation of cytochrome P450 2A6 and cytochrome P450 2A13 by menthofuran, β-nicotyrine and menthol. *Chem Biol Interact* **197:**87–92.

Murphy SE, Johnson LM, and Pullo DA (1999) Characterization of multiple products of cytochrome P450 2A6-catalyzed cotinine metabolism. *Chem Res Toxicol* **12:**639–645.

Murphy SE, Raulinaitis V, and Brown KM (2005) Nicotine 5′-oxidation and methyl oxidation by P450 2A enzymes. *Drug Metab Dispos* **33:**1166–1173.

Nakajima M, Yamamoto T, Nunoya K, Yokoi T, Nagashima K, Inoue K, Funae Y, Shimada N, Kamataki T, and Kuroiwa Y (1996) Characterization of CYP2A6 involved in 3′-hydroxylation of cotinine in human liver microsomes. *J Pharmacol Exp Ther* **277:**1010–1015.

Peterson LA, Trevor A, and Castagnoli N Jr (1987) Stereochemical studies on the cytochrome P-450 catalyzed oxidation of (*S*)-nicotine to the (*S*)-nicotine Δ1′,5′-iminium species. *J Med Chem* **30:**249–254.

Schlicht KE, Berg JZ, and Murphy SE (2009) Effect of CYP2A13 active site mutation N297A on metabolism of coumarin and tobacco-specific nitrosamines. *Drug Metab Dispos* **37:**665–671.

Shigenaga MK, Trevor AJ, and Castagnoli N Jr (1988) Metabolism-dependent covalent binding of (*S*)-[5-^{3}H]nicotine to liver and lung microsomal macromolecules. *Drug Metab Dispos* **16:**397–402.

Smith BD, Sanders JL, Porubsky PR, Lushington GH, Stout CD, and Scott EE (2007) Structure of the human lung cytochrome P450 2A13. *J Biol Chem* **282:**17306–17313.

Soucek P (1999) Expression of cytochrome P450 2A6 in *Escherichia coli*: purification, spectral and catalytic characterization, and preparation of polyclonal antibodies. *Arch Biochem Biophys* **370:**190–200.

Su T, Bao Z, Zhang QY, Smith TJ, Hong JY, and Ding X (2000) Human cytochrome P450 CYP2A13: predominant expression in the respiratory tract and its high efficiency metabolic activation of a tobacco-specific carcinogen, 4-(methylnitrosamino)-1-(3-pyridyl)-1-butanone. *Cancer Res* **60:**5074–5079.

Tuomi T, Johnsson T, and Reijula K (1999) Analysis of nicotine, 3-hydroxycotinine, cotinine, and caffeine in urine of passive smokers by HPLC-tandem mass spectrometry. *Clin Chem* **45:**2164–2172.

von Weymarn LB, Blobaum AL, and Hollenberg PF (2004) The mechanism-based inactivation of p450 2B4 by tert-butyl 1-methyl-2-propynyl ether: structural determination of the adducts to the p450 heme. *Arch Biochem Biophys* **425:**95–105.

von Weymarn LB, Brown KM, and Murphy SE (2006) Inactivation of CYP2A6 and CYP2A13 during nicotine metabolism. *J Pharmacol Exp Ther* **316:**295–303.

von Weymarn LB, Felicia ND, Ding X, and Murphy SE (1999) *N*-nitrosobenzylmethylamine hydroxylation and coumarin 7-hydroxylation: catalysis by rat esophageal microsomes and cytochrome P450 2A3 and 2A6 enzymes. *Chem Res Toxicol* **12:** 1254–1261.

von Weymarn LB and Murphy SE (2003) CYP2A13-catalysed coumarin metabolism: comparison with CYP2A5 and CYP2A6. *Xenobiotica* **33:**73–81.

von Weymarn LB, Zhang QY, Ding X, and Hollenberg PF (2005) Effects of 8-methoxypsoralen on cytochrome P450 2A13. *Carcinogenesis* **26:**621–629.

Werle E and Meyer A (1950) [Decomposition of tobacco alkaloids in animal tissue]. *Biochem Z* **321:**221–235.

Wong HL, Murphy SE, and Hecht SS (2005) Cytochrome P450 2A-catalyzed metabolic activation of structurally similar carcinogenic nitrosamines: *N*′-nitrosonornicotine enantiomers, *N*-nitrosopiperidine, and *N*-nitrosopyrrolidine. *Chem Res Toxicol* **18:**61–69.

Yano JK, Hsu MH, Griffin KJ, Stout CD, and Johnson EF (2005) Structures of human microsomal cytochrome P450 2A6 complexed with coumarin and methoxsalen. *Nat Struct Mol Biol* **12:**822–823.

Address correspondence to: Sharon E. Murphy, Masonic Cancer Center, University of Minnesota, Mayo Mail Code 806, 420 Delaware Street SE, Minneapolis, MN 55455. E-mail: murph062@umn.edu